SIMULATION COMPARISON OF PENTALINEAR WITH BILINEAR SPRING CHARACTERISTICS

SIMULATIONSVERGLEICH VON PENTALINEAREN MIT BILINEAREN FEDERKENNLINIEN

Sebastian Geiger, Jan Hofmann

Institute of Construction Materials (IWB), University of Stuttgart

SUMMARY

The paper describes investigations into the load-bearing capacity of groups of fasteners using numerical simulations (Finite element method). Initially, experimental results and simulation results by Bokor [1] are used to show the influence of different spring models. In the simulations performed [1], the load-displacement behaviour of the anchors was idealised with a pentalinear spring characteristic. Some of the simulations performed were selected and compared with simulations using a simplified spring characteristic. The aim of the study was to find out whether an idealized bilinear spring characteristic curve gives sufficiently accurate results compared to a pentalinear curve and whether it is sufficient for the evaluation of the load capacity. For this purpose, 13 anchor configurations were simulated and evaluated using both the bilinear and the pentalinear spring characteristic proposed by Bokor [1].

ZUSAMMENFASSUNG

In dieser Studie werden Untersuchungen zur Tragfähigkeit von Gruppenbefestigungen mithilfe von numerischen Simulationen (Finite-Element-Methode) beschrieben. Zunächst werden bereits durchgeführte experimentelle Ergebnisse sowie Simulationsergebnisse von Bokor [1] verwendet, um den Einfluss unterschiedlicher Federmodelle aufzuzeigen. Bei den Simulationen [1] wird das Last-Verschiebungsverhalten der Anker durch eine pentalineare Federkennlinie definiert. Einige der in [1] durchgeführten Untersuchungen wurden herangezogen, um diese mit Simulationsergebnissen unter Verwendung einer vereinfachten Federkennlinie zu vergleichen. Ziel der vorliegenden Studie ist es herauszufinden, ob durch Simulationen mit vereinfachten bilinearen Federkennlinien ausreichende

Ergebnisse erzielt werden können. Insgesamt wurden 12 Ankerplattenkonfigurationen untersucht und ausgewertet.

1. INTRODUCTION

Currently, the design of fixings in concrete is carried out in accordance with DIN EN 1992-4 [2]. Prerequisite for the application of the [2] is a linear force distribution within the anchor group. The assumption of a rigid attachment part applies, so that a linear strain distribution or force distribution analogous to the Bernoulli hypothesis is present.

To design an anchor plate, the stress in the anchor plate is determined using the von Mises-method. Neither the deformation of the anchor plate nor the displacement of the anchors themselves are taken into account in the calculation [2].

By assuming a rigid anchor plate, as is the case with the current design method [2] is used, the support forces occurring in a real group fastening can be underestimated. Due to the deformation of the anchor plate, the anchor forces can be greater compared to an absolutely rigid anchor plate. Furthermore, a linear load distribution is necessary for the design according to the CC method. In reality, despite compliance with the stress criterion, there is no linear force distribution on the anchors in a group fastening.

The non-linear spring characteristics used in this study describes the load-displacement behavior of the anchors in cracked and uncracked concrete. They are the basis for a more realistic determination of the force distribution depending on the anchor plate and connection stiffness. In combination with contact springs, which describe the behavior between the anchor plate and the concrete surface, and a flexible anchor plate, a more realistic force distribution on the anchors can be determined. This can be compared with the necessary linear force distribution.

Spring models are used in fastening technology to describe the load-displacement behavior of anchors. There are spring model approaches that describe the load-bearing behavior of the entire anchoring system and spring models that describe the behavior of individual anchors. In both cases, a distinction can be made between linear and non-linear spring models. Linear spring models use a stiffness, which leads to an excessive stiffness of anchors being assumed in the failure area. Non-linear spring models describe the anchor behavior using variable stiffnesses. These can be defined up to the post-failure range and describe the real anchor behavior much more accurately.

A spring model can be used to describe the load-displacement behavior of anchors in an abstract manner. Spring characteristics can be derived for tensile and shear loads and take different influencing factors into account. However, the basis for every spring model is to resolve the mutual influence of the springs so that the spring characteristics are only influenced by "external" boundary conditions. In this work, a bilinear spring model approach for centric tension is used without modeling a post-breakage range.

It is investigated whether sufficiently accurate results can be achieved with a simplified bilinear spring characteristic curve without post-breakage range.

2. STATE OF THE ART

Fastening systems are currently designed on the assumption of a rigid anchor plate. There are two points that can lead to an unsafe design.

1. If the anchor plate is deformed, additional forces acting on the anchors are neglected or underestimated. The DIN EN 1992-4 points out that these must be taken into account in the assessment, although the procedure is not described in detail.
2. The load-bearing capacity of anchor groups is calculated assuming a linear load distribution. In the case of a non-linear force distribution due to a flexible anchor plate, the loads acting on the individual anchors can be significantly higher than with a linear force distribution.

Studies on the stiffness behavior of anchor plates are summarized in [3] and [4]. In [1] the problem of a rigid anchor plate is investigated by means of tests with different anchor plate thicknesses. Fig. 1 and Fig. 2 shows the load-bearing capacities of a 4x1 anchor group used in [1] was investigated. A lower anchor plate stiffness also results in a lower load-bearing capacity of the anchor group. A thicker anchor plate, as shown in Fig. 2 a), distributes the acting force better over the anchors of the group than a thin anchor plate, as shown in Fig. 2 c). With a thick anchor plate, the load is applied more evenly and all anchors are activated simultaneously. In contrast, with a thinner anchor plate, as shown in Fig. 2 c), the anchors are activated one after the other, which means that the middle anchor must fail first for a load redistribution (see Fig. 2 d)). This leads to a lower load-bearing capacity of the anchor group.

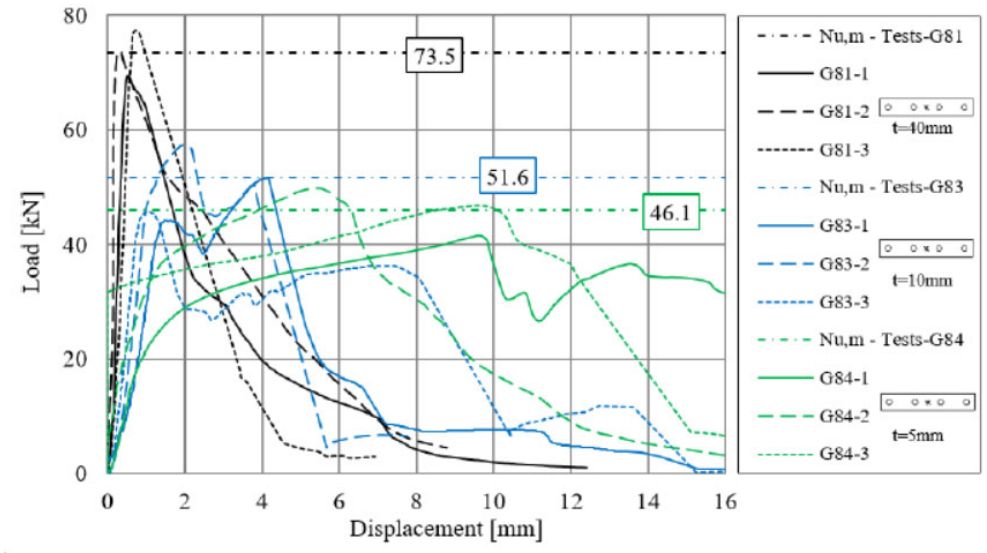

Fig. 1: Influence of the anchor plate thickness on the load-bearing capacity [1]

Fig. 2: Influence of the anchor plate thickness (stiffness) on the anchor group a) anchor plate with sufficiently stiff anchor plate G81 (d = 40mm); b) break-out body G81; c) anchor plate with flexible anchor plate G83 (d = 10mm); d) break-out body G83; e) thin anchor plate G84 (d = 5mm) [1]

The assumption of a rigid anchor plate is difficult to achieve in practice. Therefore, the interactions between anchor plate, anchor and connection profile must be taken into account. To make this possible, spring characteristics are required that describe the load-displacement behavior of a single anchor with sufficient accuracy.

In linear spring models, the anchor behavior is described with constant stiffness without a break-off criterion. Such spring models are realistic for actions in which the anchoring system behaves linearly elastically. This is usually the case up to a load level of 30 % to 50 % of the breaking load. The secant stiffness of the anchors can be used from tests when 50 % of the load-bearing capacity is reached. Such spring models are used in fastening technology to determine the load distribution on the anchors for a design load.

The multilinear spring characteristics, on the other hand, are used to describe the entire load-bearing behavior, far into the post-cracking range. For this purpose, the decrease in stiffness at a load of more than 50 % of the load-bearing capacity is taken into account. In addition, the softening behavior in the post-cracking area of the anchors can also be taken into account. Such models can be used, for example, to determine the load-bearing capacity of a group of anchors. In addition, these models can realistically describe the interactions between the supporting structure and the anchorage [5, 6].

Due to their complexity, nonlinear spring models with modeling of the post-failure behavior have been used either for performance evaluation of specific cases or for research and development. Considering the complexity of the modeling approach and a variety of possible definitions of spring properties and fracture criteria, the procedure for integrated FE models of anchor plate systems has not yet been introduced in guidelines.

The calculation of the anchor loads using spring models and real anchor plate stiffness results in a non-linear force distribution, which in some cases makes it impossible to use the CC method safely. The non-linear distribution of the anchor loads can therefore be dealt with in two different ways.

1. the anchor plate thickness must be increased to such an extent that the anchor loads correspond to those determined in compliance with the Bernoulli hypothesis.

2. the linear anchor loads are increased with an α-factor until each anchor in the group deviates by a maximum of x % from the force that was determined in compliance with the Bernoulli hypothesis. This α-factor describes the ratio between the anchor force with a sufficiently stiff and insufficiently stiff anchor plate.

In case 2, the procedure is such that the specified anchor plate thickness is initially retained. Then all calculated anchor loads for the rigid anchor plate are increased with the α factor. This takes into account a maximum load increase resulting from the non-linear force distribution. At the same time, the linear force distribution according to [2] is ensured. The disadvantage of this method is that the sum of the tensile and compressive forces acting on the anchors no longer corresponds to the acting load.

A schematic force distribution is shown below for a rigid anchor plate in Fig. 3 a) and a flexible anchor plate in Fig. 3 b). Fig. 3 c) shows the result of the anchor loads multiplied by the α factor (α = 14 kN/10 kN = 1.4).

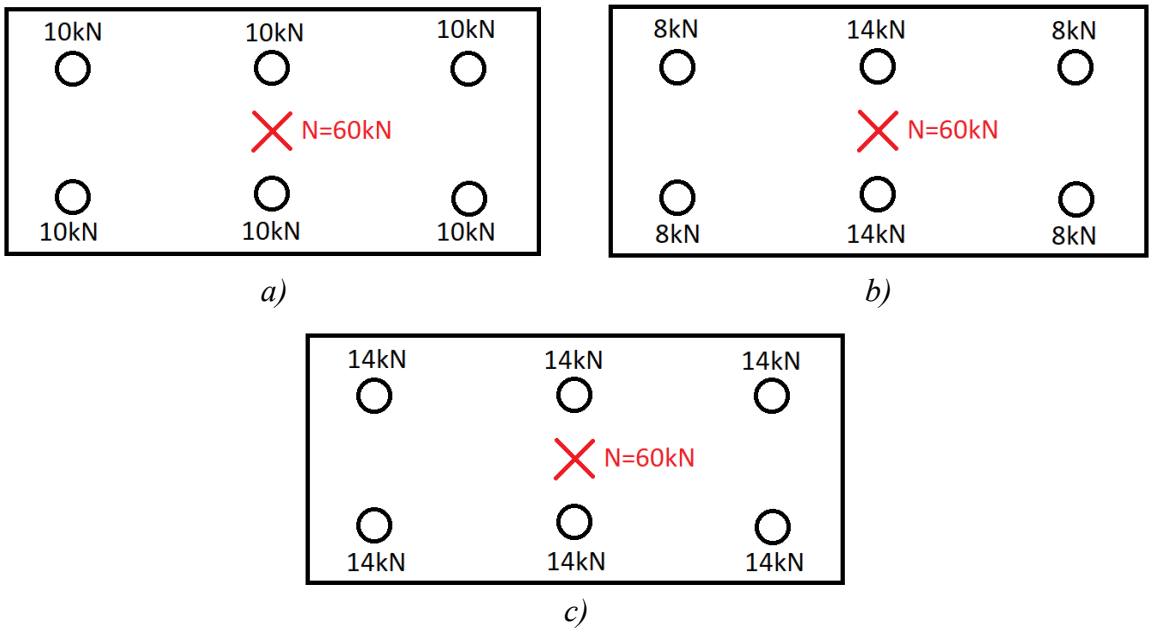

Fig. 3: Load distribution with rigid and flexible anchor plate a) linear force distribution with rigid anchor plate; b) non-linear force distribution with flexible anchor plate c) load increase using α factor to take non-linear force distribution into account

3. MODELLING

The finite element software ANSYS® [7] is used for the numerical investigations, with which a static-mechanical analysis is carried out.

Shell and solid elements are used for the geometry modeling. For this purpose, the offset type of the anchor plate, the steel profile and the anchor base are each placed in the center of the shell elements. The steel properties are described using bilinear isotropic hardening, in which the yield strength is set to 235 MPa and the tangent modulus to 0 MPa.

The concrete substrate is modeled as rigid solid. This solid is fixed to the reference coordinate system. In addition, the contact surface between the anchor plate and the concrete surface is defined as frictionless. This frictionless contact surface simulates the behavior of the concrete under compressive loading, using the pure-penalty method with a normal stiffness value of 150 N/mm².

The anchors are simulated by springs. The COMBIN39 element type is used to define the spring properties. The movable end is fixed to the anchor plate and the other side of the element is fixed to the coordinate system. The springs can only absorb tensile forces, whereby the degrees of freedom of the elements are restricted to such an extent that movement is only possible in a vertical direction. To stabilize the system, additional horizontal springs were attached in the x and z directions. The horizontal springs have the same tensile and compressive stiffnesses. The meshing of the model is carried out automatically by the program, whereby the element size was set to 8 mm. The load on the system is applied displacement-controlled.

4. VALIDATION

At the beginning of the investigations, results from [1] are used to obtain a comparison with calculations. The same spring characteristics used for modeling in [1] were used in the new calculations. The G65 and G66 series are considered below (see Fig. 4 and Fig. 5). All configurations investigated according to [1] are shown in Fig. 10.

The G65 and G66 series is a 3x1 anchor plate with a thickness of 50 mm under eccentric tensile load. One anchor of the group is influenced by a crack. The other two anchors are anchored in non-cracked concrete. Fig. 4 and Fig. 5 show the test

results as a load-displacement curve, the results of the simulations using the pentalinear spring characteristic curve in [1] (SAP2000) and the pentalinear spring characteristic curve of the comparative calculations (ANSYS). The results of the FE simulation are in high agreement with the test results up to the failure load. A deviation can only be seen in the post-failure behavior. Despite the same modeling of the two FE simulations, there are differences here which are presumably due to the different boundary conditions or solvers.

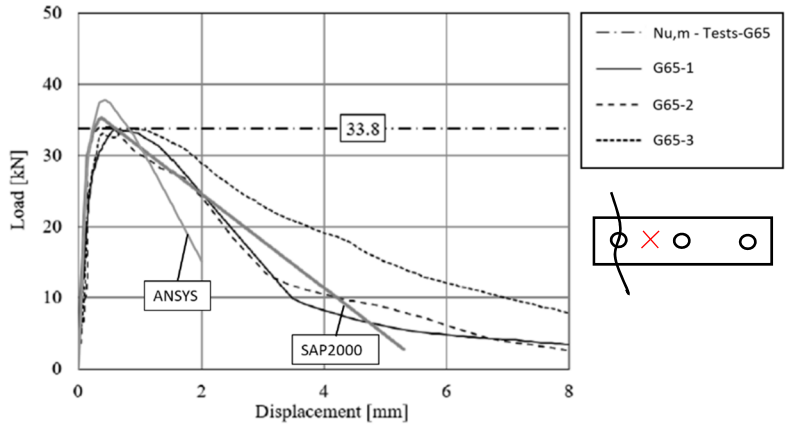

Fig. 4: Load-displacement curve of the G65 series, based on [1]

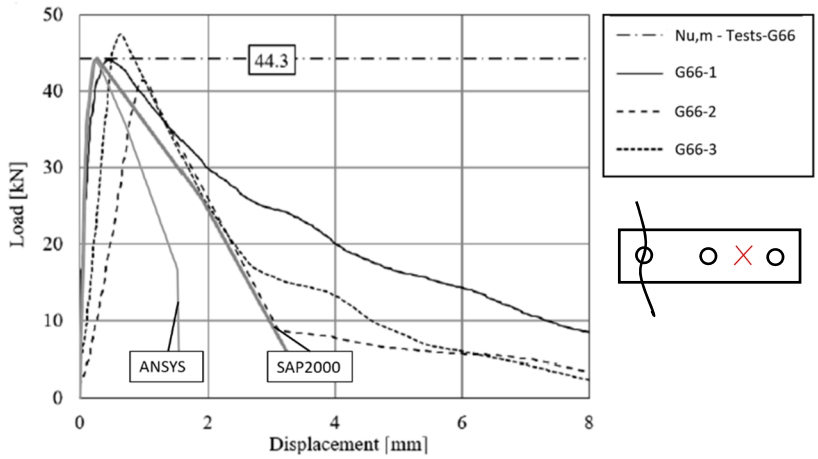

Fig. 5: Load-displacement curve of the G66 series, based on [1]

Despite the existing differences, the agreement of the simulation results can be considered good, so that [7] is used for further investigations. However, it should be noted that when using the post-breakage range, e.g. to take into account a load redistribution within a group, different group load capacities are determined even with different FE programs but the same definition of the spring characteristics.

5. DERIVATION OF THE BILINEAR SPRING CHARACTERISTIC CURVE

The basis for deriving a bilinear spring characteristic curve are the existing pentalinear spring characteristic curves from [1].

The spring characteristics refer to a single anchor and do not include any mutual interaction. Therefore, they are adapted and scaled via the projected area and the resulting reduction factor $A_{c,Ni}$ /$A_{c,N}$. The reduction depends on the edge and center distance, whereby the areas are calculated assuming equal loading of all anchors.

Furthermore, a distinction is made between anchors that are anchored in cracked concrete and non-cracked concrete. Anchors that are anchored in cracked concrete have a greater displacement with a lower load-bearing capacity, which is also taken into account by a scaling factor.

In order to simplify the calculation and definition of the spring characteristics, a bilinear spring characteristic is derived from the pentalinear spring characteristics. It is then shown that this simplification has only a minor effect on the accuracy of the calculation. The derivation rules for the bilinear spring characteristic curve are defined as follows:

1. the first point (A) is at the origin (0/0).
2. the second point (B) at 0.8 $N_{u.m}$. This means that the first two points A and B remain unchanged compared to the pentalinear spring characteristic curve.
3. the third point (C) of the bilinear spring characteristic curve is placed between the two points C and D of the pentalinear spring characteristic curve. The point is therefore in the middle of the plateau defined in the pentalinear spring characteristic curve.
4. the last point D is defined in such a way that no more load can be applied once the maximum load has been reached. This means that the displacement is the same as at point (C) and the force is set to 0 kN.

The following table shows the definition points of the spring characteristics for the bilinear format.

Table 1: Derivation of bilinear spring characteristics from pentalinear spring characteristics in non-cracked concrete for series G61 to G68

G61-G68 uncracked - pentalinear

Anchor A1 and A3 (outer)	Load [kN]	Stiffness [kN/mm]	Displacement [mm]
A	0,0	0,0	0,00
B	18,5	191,8	0,10
C	23,1	116,3	0,20
D	23,1	78,1	0,30
E	4,6	2,4	1,91
F	0,0	0,0	1,91

Anchor 2 (middle)	Load [kN]	Stiffness [kN/mm]	Displacement [mm]
A	0,0	0,0	0,00
B	14,8	191,8	0,08
C	18,5	116,3	0,16
D	18,5	78,1	0,24
E	3,7	2,4	1,53
F	0,0	0,0	1,53

G61-G68 uncracked - bilinear

Anchor A1 and A3 (outer)	Load [kN]	Stiffness [kN/mm]	Displacement [mm]
A	0,0	0,0	0,00
B	18,5	191,8	0,10
C_1	23,1	92,4	0,25
D_1	0,0	0,0	0,26

Anchor 2 (middle)	Load [kN]	Stiffness [kN/mm]	Displacement [mm]
A	0,0	0,0	0,00
B	14,8	191,8	0,08
C	18,5	92,4	0,20
D	0,0	0,0	0,21

Table 2: Derivation of bilinear spring characteristics from pentalinear spring characteristics in non-cracked concrete for series G61 to G68

G61-G68 cracked - pentalinear

Anchor A1 and A3 (outer)	Load [kN]	Stiffness [kN/mm]	Displacement [mm]
A'	0,0	0,0	0,00
B'	12,8	82,1	0,17
C'	16,0	38,6	0,41
D'	16,0	30,6	0,52
E'	3,2	1,2	2,71
F'	0,0	0,0	2,71

Anchor 2 (middle)	Load [kN]	Stiffness [kN/mm]	Displacement [mm]
A	0,0	0,0	0,00
B	10,2	82,1	0,14
C	12,8	38,6	0,33
D	12,8	30,6	0,42
E	2,6	1,2	2,17
F	0,0	0,0	2,17

G61-G68 cracked - bilinear

Anchor A1 and A3 (outer)	Load [kN]	Stiffness [kN/mm]	Displacement [mm]
A'	0,0	0,0	0,00
B'	12,8	82,1	0,17
C'_1	16,0	34,0	0,47
D'_1	0,0	0,0	0,48

Anchor 2 (middle)	Load [kN]	Stiffness [kN/mm]	Displacement [mm]
A	0,0	0,0	0,00
B	10,2	82,1	0,14
C	12,8	34,0	0,38
D	0,0	0,0	0,39

Table 3: Derivation of bilinear spring characteristics from pentalinear spring characteristics in cracked concrete for series G81, G82, G83

G81-G83 uncracked -pentalinear

Anchor A1 and A4 (outer)	Load [kN]	Stiffness [kN/mm]	Displacement [mm]
A	0,0	0,0	0,00
B	20,6	97,8	0,21
C	25,7	65,2	0,39
D	25,7	47,1	0,55
E	5,1	2,4	2,18
F	0,0	0,0	2,18

Anchor A2 and A3 (middle)	Load [kN]	Stiffness [kN/mm]	Displacement [mm]
A	0,0	0,0	0,00
B	13,7	97,8	0,14
C	17,1	65,2	0,26
D	17,1	47,1	0,36
E	3,4	2,4	1,46
F	0,0	0,0	1,46

G81-G83 uncracked - bilinear

Anchor A1 and A4 (outer)	Load [kN]	Stiffness [kN/mm]	Displacement [mm]
A	0,0	0,0	0,00
B	20,6	97,8	0,21
C	25,7	54,7	0,47
D	0,0	0,0	0,48

Anchor A2 and A3 (middle)	Load [kN]	Stiffness [kN/mm]	Displacement [mm]
A	0,0	0,0	0,00
B	13,7	97,8	0,14
C	17,1	54,7	0,31
D	0,0	0,0	0,32

To illustrate this, the spring characteristics of the outer anchors for the G61 to G68 series are shown both in pentalinear format and in bilinear format (see Fig. 6).

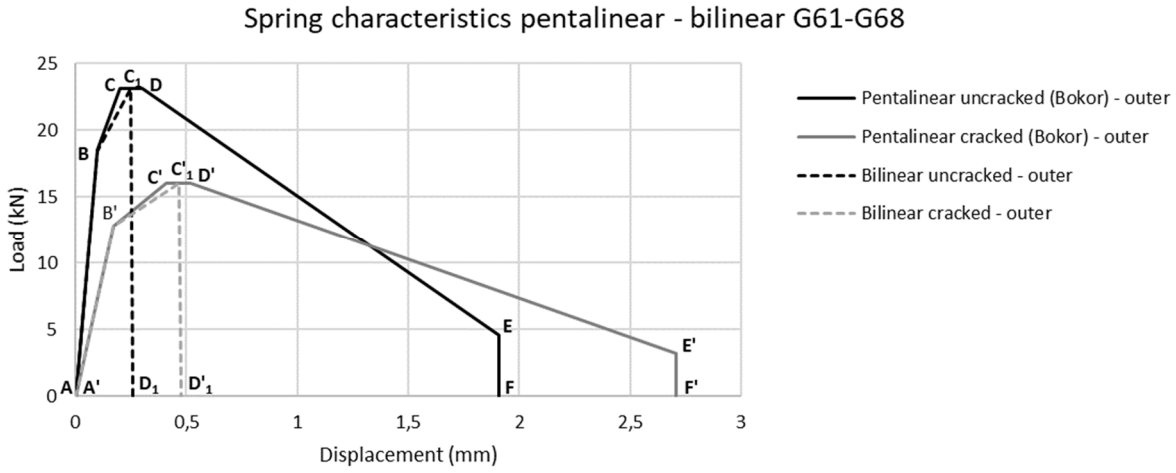

Fig. 6: Comparison of bilinear and pentalinear spring characteristics

5.1 Investigated Configurations

A total of 12 different group anchorages with bonded anchors, which have already been investigated in [1], are simulated. Group anchorages with two different anchor plate geometries, different load application points and different crack configurations are considered. All group anchorages are simulated with bilinear and pentalinear spring characteristics. The results of the investigations are compared with the tests and the simulation results from [1].

In order to determine the sensitivity of the displacement at 50 % of the maximum load, the influence of modified bilinear spring characteristics on the simulation results is investigated in further calculations. For this purpose, point B is shifted downwards to a value of 0.5 $N_{u.m}$ or 0.3 $N_{u.m}$ respectively. The initial stiffness remains identical in each of the simulations. The stiffness between points B and C increases as a result. Furthermore, point C is shifted so that the maximum deformation varies when the maximum load is reached. Point C is selected so that it lies at the beginning, middle and end of the plateau of the pentalinear spring characteristic [1]. An overview of the spring characteristics used for the parameter study is shown in Fig. 7.

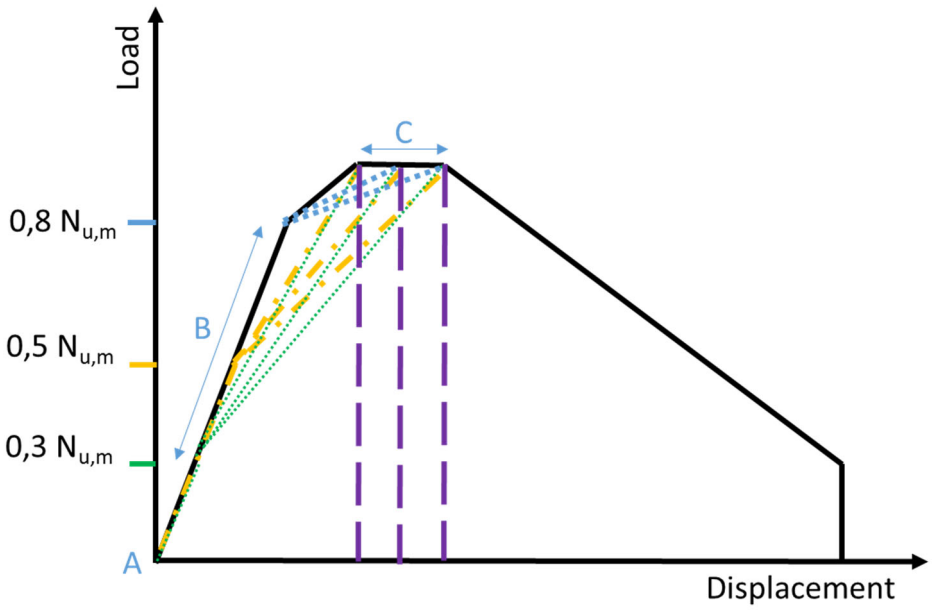

Fig. 7: Modified bilinear spring characteristics

An overview of the configurations examined is shown in Fig. 8. The nomenclature was adopted from [1] to simplify the comparison.

Series	Configuration	Size lxwxh [mm]	Anchor distance s_1 [mm]
G61		400x120x50	120
G62R		400x120x50	120
G62		400x120x50	120
G63		400x120x50	120
G64		400x120x50	120
G65		400x120x50	120
G66		400x120x50	120
G67		400x120x50	120
G68		400x120x50	120
G81		350x60x40	90
G82		350x60x40	90
G83		350x60x10	90

Fig. 8: Investigated configurations

6. RESULTS OF SIMULATION AND DISCUSSION

A total of 12 anchor plate configurations are examined. The load-displacement behavior with pentalinear spring characteristics according to [1], which is calculated with [7], is shown as a black curve in the following diagrams. Further simulation results with pentalinear spring characteristics according to [1] are available for the G65, G66, G81, G82 and G83 series. These results according to [1] are shown as red curves in the corresponding diagrams.

The simulation results with bilinear spring characteristics are shown as blue lines. The evaluation of these simulation results shows a very good agreement of the load-displacement behavior up to the maximum load-bearing capacity of the configurations G61 - G68. Both the maximum loads and the corresponding displacements are in good agreement with the experimental results. Since the post-failure behavior is not modeled in the definition of the bilinear spring characteristics, the simulation results show a planned steep load drop that occurs after the maximum load is reached.

Fig. 9 shows the relationship between the maximum loads of simulations with a bilinear spring characteristic curve and the load capacities of the experimental results. There is good agreement between the simulation results and the test results across all series. For the G81 - G83 series, the simulation results are slightly below the experimental results. Looking at all 12 series, the simulation results are generally lower than the experimental results. Table 4 provides an overall ratio of 0.94 with a coefficient of variation of 13.7 %.

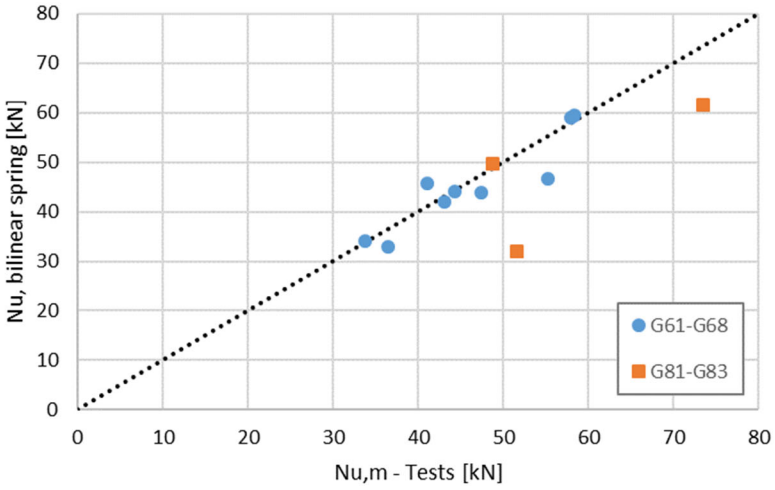

Fig. 9: Relationship between the simulation results of bilinear spring characteristics and experimental results

If the result is adjusted for series G83, the overall ratio is 0.97. The overall ratio of the simulations with pentalinear spring characteristics [1] is 0.98 with a coefficient of variation of 8.5 %. The evaluation of the simulation results with bilinear spring characteristics shows that the calculated results are on the safe side compared to the test results. The coefficient of variation of the ratio of the bilinear spring characteristics to the test results is approx. 14 % higher than when using pentalinear spring characteristics. This deviation is due to the neglect of the post-breakage range, where the accuracy decreases and the maximum load is lower for group anchorages, as there is no load redistribution.

Table 4: Overall ratio of the investigated series: Experimental results - pentalinear simulation results [1]; experimental results - bilinear simulation results

Serie:	Experiment: $N_{u,m}$ [kN]	Bokor: $N_{u,\ pentalinear}$ [kN]	*Nu,pentalinear / $N_{u,m}$ [-]*	Diese Studie: $N_{u,\ bilinear}$ [kN]	*Nu,bilinear / $N_{u,m}$ [-]*
G61	58,4	62,6	1,07	59,4	1,02
G62	58,0	59,1	1,02	59,0	1,02
G62-R	43,1	44,1	1,02	42,0	0,97
G63	41,0	43,9	1,07	45,7	1,12
G64	55,3	49,5	0,90	46,6	0,84
G65	33,8	35,2	1,04	34,1	1,01
G66	44,3	44,3	1,00	44,1	0,99
G67	47,4	47,4	1,00	44,0	0,93
G68	36,5	32,1	0,88	33,0	0,90
G81	73,5	76,2	1,04	61,6	0,84
G82	48,8	45,5	0,93	49,7	1,02
G83	51,6	41,8	0,81	31,9	0,62
	Mittelwert:		**0,98**		**0,94**
	Standardabweichung:		**0,08**		**0,13**
	Variationskoeffizient:		**8,48%**		**13,73%**

The results for the simulation of the G61 series with pentalinear spring characteristics [1] are higher than determined by the experiments. The post-breakage behavior is flatter. The results of the simulations with a bilinear spring characteristic curve provide very good agreement compared to the experimental results. However, the overall behavior with bilinear spring characteristics is stiffer than with pentalinear spring characteristics. This stiffer behavior results from the assumed spring characteristic curve, which does not show a plateau at the maximum load compared to the pentalinear spring characteristic curves [1]. The simulation results for the investigated series are shown in Fig. 10 and show very good agreement with the experiments.

For the G83 series, there is less agreement between the experimental and simulation results. This applies both to the results with the bilinear and the pentalinear

spring characteristics. The maximum load determined for both spring characteristics is below the experimental failure load. Presumably, the original calculation with the SAP2000 software from Bokor selected boundary conditions that neglect the resulting shear forces in the system.

Fig. 10 shows all the series investigated using a simplified bilinear spring characteristic curve. The diagrams show the actual and simulated load-displacement curves.

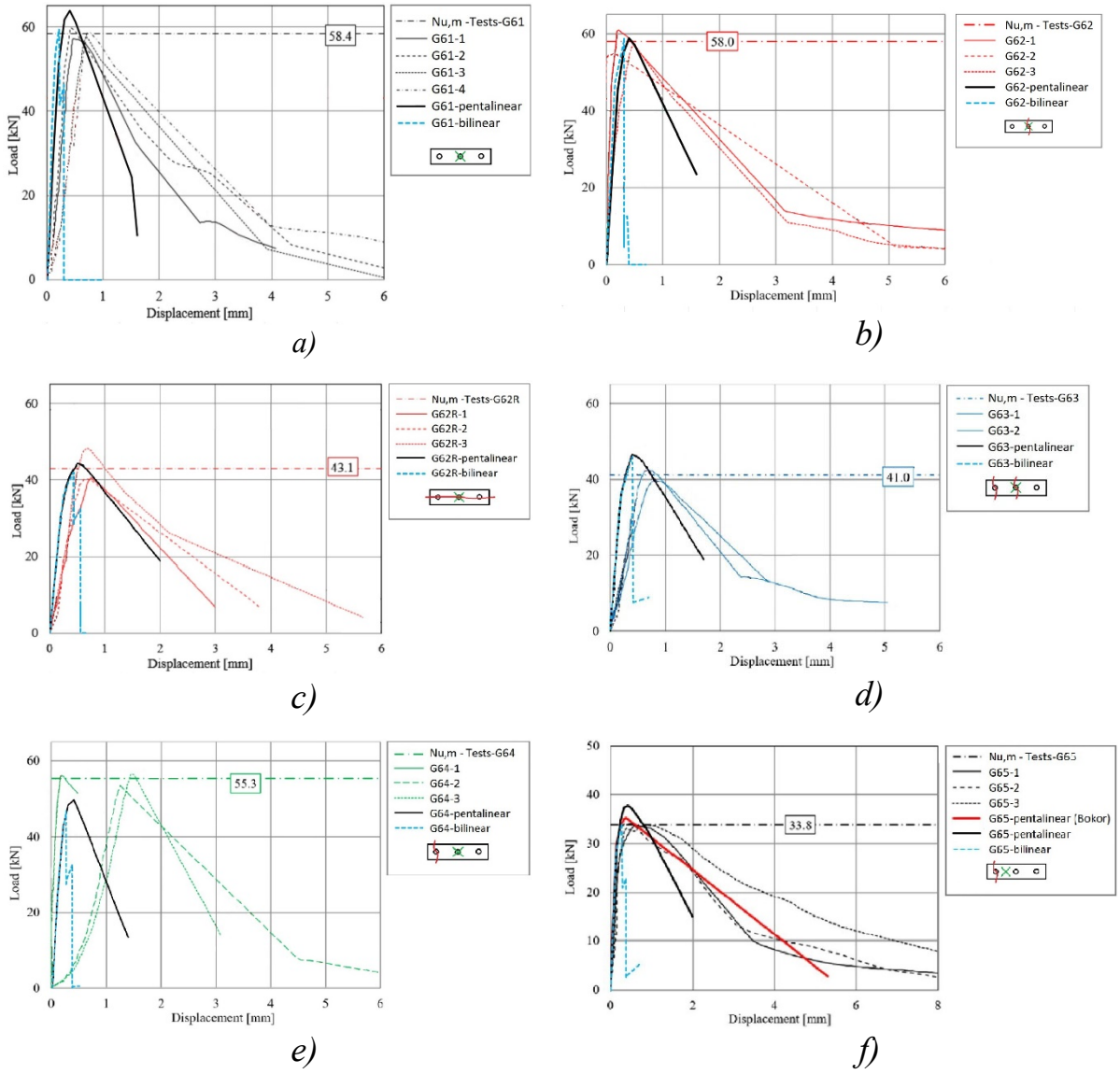

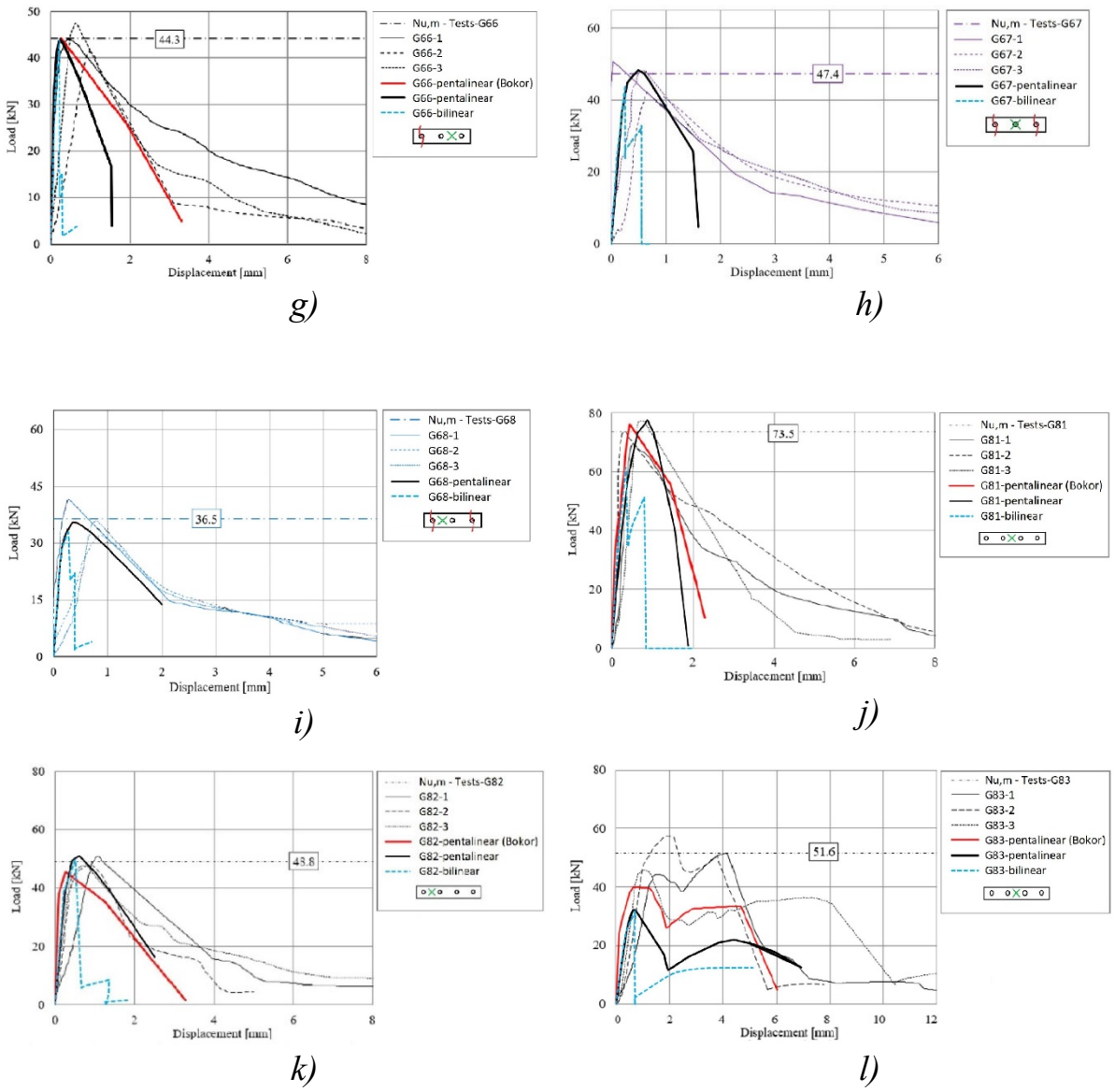

Fig. 10: Test results and simulation results series G61 - G83, based on [1]

Further investigations were carried out to determine the effect of a change in the bilinear spring characteristic curve in Fig. 7. Modified bilinear spring characteristics were assumed for this purpose. The procedure for deriving these modified spring characteristics and the findings are shown below.

First, point B is modified and the height of $0.8N_{u,m}$ is varied by shifting it to the load levels of $0.5N_{u,m}$ and $0.3N_{u,m}$. In the work of [1], the choice of $0.8N_{u,m}$ is justified by the fact that most anchors have a constant initial stiffness up to this load. The selected initial stiffness is the secant stiffness at $0.5N_{u,m}$.

Point B at $0.3N_{u,m}$ is freely selected in this study. It is assumed that concrete generally behaves linearly elastic up to a load level of 30 %. This means that an anchorage normally behaves linearly elastic up to a load level of $0.3N_{u,m}$.

Fig. 11 shows the described modification of the bilinear spring characteristic.

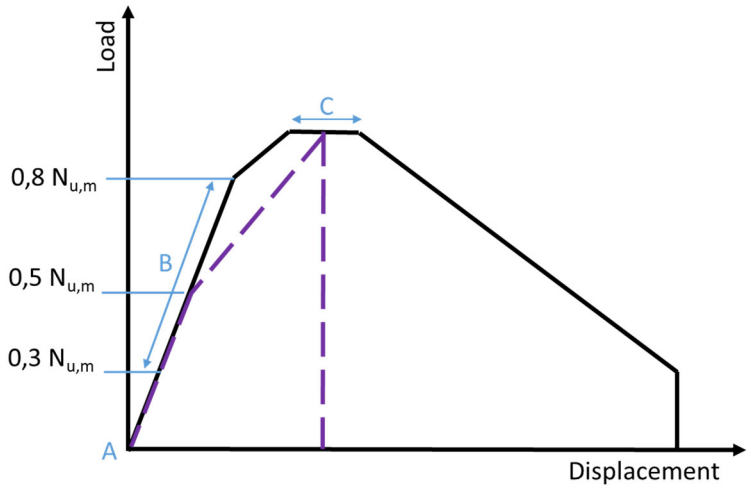

Fig. 11: Parameter study: Variation of point B of the bilinear curve

The results of the simulations show that the load-bearing capacity of the anchor groups decreases the further point B is moved. The investigations also show that the results change only slightly if point B is moved upwards or downwards. Based on these findings, point B is set at $0.5N_{u,m}$ for the further investigations. The load and the displacement at 50 % of the maximum load ($0.5N_{u,m}$) are also known from most tests and are measured and evaluated as standard.

Table 5: Total ratio variation point B: experimental results - bilinear simulation results

Series:	Experiment: $N_{u,m}$ [kN]	$N_{u,\,bilinear,\,0.8}$ [kN]	$N_{u,\,bilinear,\,0.8}$ / $N_{u,m}$ [-]	$N_{u,\,bilinear,\,0.5}$ [kN]	$N_{u,\,bilinear,\,0.5}$ / $N_{u,m}$ [-]	$N_{u,\,bilinear,\,0.3}$ [kN]	$N_{u,\,bilinear,\,0.3}$ / $N_{u,m}$ [-]
G61	58,4	59,4	1,02	54,8	0,94	51,7	0,89
G62	58,0	59,0	1,02	57,8	1,00	57,3	0,99
G62-R	43,1	42,0	0,97	39,3	0,91	38,0	0,88
G63	41,0	45,7	1,12	45,1	1,10	44,5	1,08
G64	55,3	46,6	0,84	41,8	0,76	38,9	0,70
G65	33,8	34,1	1,01	33,3	0,99	30,8	0,91
G66	44,3	44,1	0,99	43,4	0,98	43,1	0,97
G67	47,4	44,0	0,93	37,7	0,80	34,7	0,73
G68	36,5	33,0	0,90	30,7	0,84	29,6	0,81
G81	73,5	61,6	0,84	60,3	0,82	58,4	0,79
G82	48,8	49,7	1,02	49,4	1,01	45,0	0,92
G83	51,6	31,9	0,62	32,2	0,62	32,3	0,63
	Average:		**0,94**		**0,90**		**0,86**
	Standard deviation		**0,13**		**0,13**		**0,13**
	Coefficient of variation		**13,73%**		**14,83%**		**15,28%**

A further modification of the bilinear spring characteristic curve is made at point C. In this area, a plateau is defined in the pentalinear curve, which is omitted in the bilinear spring characteristic curve. The tests are used to investigate the influence of point C of the bilinear spring characteristic curve. This is assumed to be at the beginning, end and middle of this plateau and the load-bearing capacity of the different anchor plate configurations is investigated. Fig. 12 shows the three investigated spring characteristics schematically.

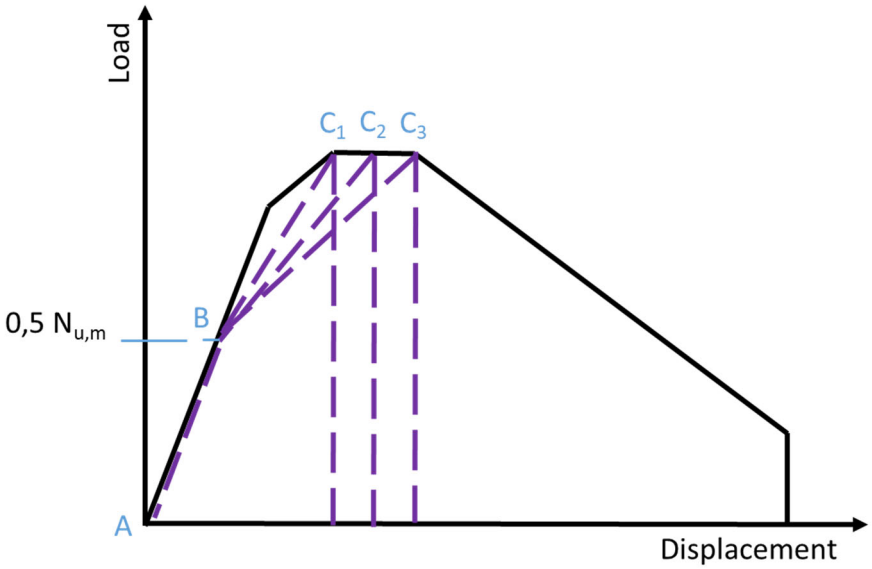

Fig. 12: Parameter study: Variation of point C of the bilinear curve

When comparing the load-bearing capacities, the results with the bilinear spring characteristic curve and point C2 provide the smallest deviations. Both the stiffer curve (C1) and the softer curve (C3) provide lower load-bearing capacities on average. Table 6 contains all the simulation results and describes the change that occurs with the position of point C.

Table 6: Total ratio variation point C: experimental results - bilinear simulation results

Series:	Experiment: $N_{u,m}$ [kN]	$N_{u,bilinear,C1}$ [kN]	$N_{u,bilinear,C1}$ / $N_{u,m}$ [-]	$N_{u,bilinear,C2}$ [kN]	$N_{u,bilinear,C2}$ / $N_{u,m}$ [-]	$N_{u,bilinear,C3}$ [kN]	$N_{u,bilinear,C3}$ / $N_{u,m}$ [-]
G61	58,4	49,6	0,85	54,8	0,9385	54,6	0,93
G62	58,0	57,5	0,99	57,8	0,9972	58,6	1,01
G62-R	43,1	38,8	0,90	39,3	0,9126	39,6	0,92
G63	41,0	44,7	1,09	45,1	1,1007	44,7	1,09
G64	55,3	38,7	0,70	41,8	0,7557	42,5	0,77
G65	33,8	31,9	0,94	33,3	0,9855	33,6	0,99
G66	44,3	41,0	0,93	43,4	0,9797	42,7	0,96
G67	47,4	35,7	0,75	37,7	0,7954	38,5	0,81
G68	36,5	29,3	0,80	30,7	0,8419	32,0	0,88
G81	73,5	58,1	0,79	60,3	0,8208	52,1	0,71
G82	48,8	46,2	0,95	49,4	1,0115	49,4	1,01
G83	51,6	31,9	0,62	32,2	0,6246	32,0	0,62
	Average:		**0,86**		**0,90**		**0,89**
	Standard deviation		**0,13**		**0,13**		**0,14**
	Coefficient of variation		**15,52%**		**14,83%**		**15,67%**

7. SUMMARY

The use of simplified bilinear spring characteristics describes the load-displacement behavior of the group fastenings investigated here sufficiently accurately and the simulation results deviate little from the results with a pentalinear spring characteristic. It is also possible to obtain a sufficiently good estimate of the load-bearing capacity without defining the post-failure behavior and a simple bilinear spring characteristic. The investigations show a good agreement between experimental results and numerical simulations when using the bilinear spring models without post-failure area or load plateau. Point B has a moderate influence on the determined load capacities. A lower position of point B leads to a lower load-bearing capacity of the anchor group, a higher position of point B leads to higher load-bearing capacities of the anchor group. The results are summarized in Fig. 13.

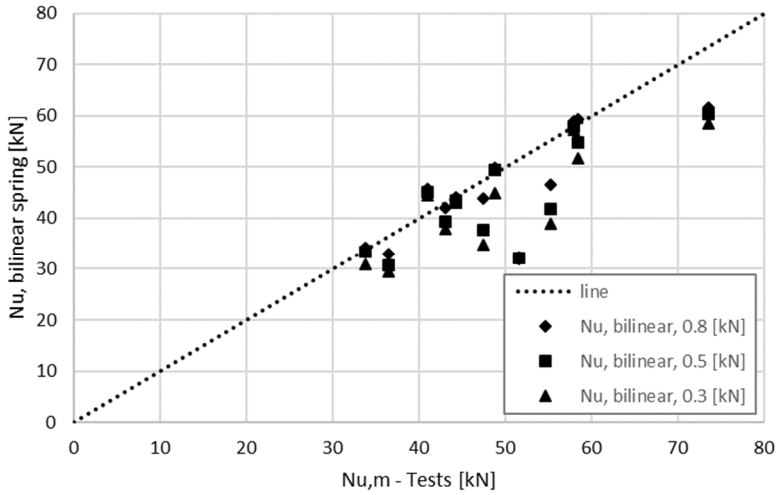

Fig. 13: Parameter study: overall representation of the variation of point B: experimental results and bilinear simulation results

Point C also has an influence on the load-bearing capacity. However, this influence is significantly less than the position of point B. Fig. 14 summarizes the results.

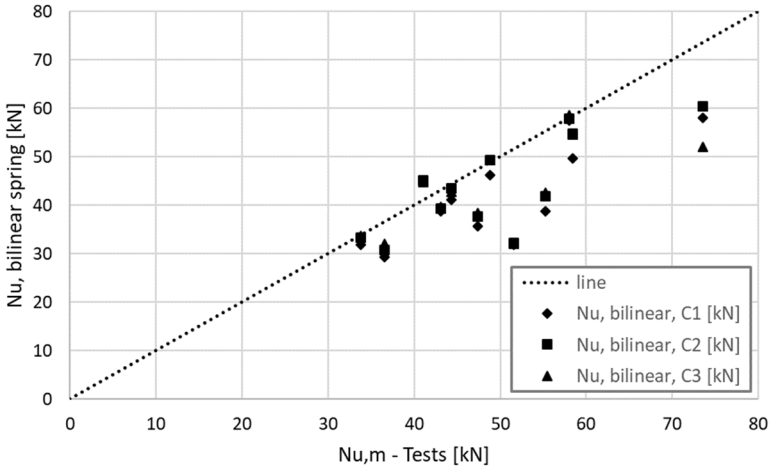

Fig. 14: Parameter study: Overall representation of the variation of point C: experimental results & bilinear simulation results

All spring models currently used are not covered by standardized regulations, e.g. in the LBO [8] or EN 1992-4 [2]. The use of a flexible anchor plates is also not currently regulated or described. Various working groups are currently working on a regulation to include spring models for the modeling of anchorages and the calculation with flexible anchor plates in a normative regulation. There are still a number of unanswered questions that need to be answered before inclusion. For example, it still needs to be clarified how the different types of failure can be taken

into account in a single spring model. There is also the question of how the spring characteristics can be determined in a "standardized way" so that they can be derived as product-dependent design parameters.

There are still some important questions that need to be answered before spring models can become an integral part of fastening technology design.

REFERENCES

[1] BOKOR, B.: *Nonlinear spring modelling approach for the evaluation of anchor groups*. Doctoral Thesis, Universität Stuttgart, 2021, http://elib.uni-stuttgart.de/handle/11682/11578

[2] DIN EN 1994-2: *Eurocode 2 - Bemessung und Konstruktion von Stahlbeton- und Spannbetontragwerken – Teil 4: Bemessung der Verankerung von Befestigungen in Beton*. Epub ahead of print 2019. DOI: 10.31030/1719423

[3] LI, L.: *Required Thickness of Flexurally Rigid Baseplate for Anchor Fastenings*. High Tech Concr Technol Eng Meet 2018; 938–947

[4] MALLÉE, R., BURKHARDT, F.: *Befestigungen von Ankerplatten mit Dübeln - Ein Beitrag zur erforderlichen Ankerplattendicke*. Beton- Stahlbetonbau 1999; 94: 502–511

[5] HOFMANN, J., MAHADIK, V., SHARMA, A.: *Modelling structure-anchor-component interaction fpr nuclear safety related structures under seismic loads - Part 2: development of numerical Model*. Transactions, SMiRT-23, Manchester, United Kingdom, August 10-14, 2015

[6] DWENGER, F.: *Einfluss des Tragverhaltens von Dübelbefestigungen auf die Bauwerk-Komponenten-Wechselwirkungen bei Erdbebenbeanspruchung.* Doctoral Thesis, Universität Stuttgart, 2019 http://elib.uni-stuttgart.de/handle/11682/10257

[7] ANSYS®, 2022R1. Academic Researchh Mechanical, Release 2022R1

[8] Landesbauordnung für Baden-Württemberg (LBO). 2023